Orbit Following Calculation of Energetic Ions in the Design of Ferritic Insertion in the JT-60U

Kouji SHINOHARA, Yutaka SUZUKI, Shinji SAKURAI, Kei MASAKI, Takaaki FUJITA and Yukitoshi MIURA

Fusion Research and Development Directorate, Japan Atomic Energy Agency, Naka 311–0193, Japan

(Received 28 November 2005 / Accepted 12 January 2006)

The design process regarding ferritic insertion in the JT-60U is described from the viewpoint of the behavior of energetic ions. The confinement of energetic ions and the absence of unfavorable heat flux on the first wall were assessed using the Fully Three-Dimensional magnetic field OFMC code, which was developed for the toroidal field ripple reduction experiment program utilizing ferritic inserts in the JFT-2M. In the final design, the absorbed power in the neutral beam injection is improved by a factor of about 1.3 in a large volume plasma with $B_{t_0} = 1.9$ T.

© *2006 The Japan Society of Plasma Science and Nuclear Fusion Research*

Keywords: JT-60U, tokamak, ferritic steel, ripple reduction, F3D OFMC, high energetic ion, JFT-2M

DOI: 10.1585/pfr.1.007

1. Introduction

On a tokamak, in order to leave space for ports for neutral beams, diagnostics, the vacuum system and so on, 16 – 32 coils are distributed to produce toroidal magnetic field (TF). Because of its discreteness, such coil system produces TF ripple. The TF ripple induces loss of energetic ions due to local mirror trapping (ripple trapped loss) or due to the lack of the up-down symmetry of banana orbit (banana diffusion). These losses reduce the "effective" efficiency of plasma heating through reducing the number of confined energetic particles. This loss also can affect the confinement of bulk plasma as was observed in the JET [1]. Additionally, the ripple trapped loss of energetic particles creates a large localized heat load on the first wall, which could induce an unacceptable heat load for the material of the first wall [2–4]. Thus, the TF ripple was one of important issues in the ITER design and has been investigated by many authors [5–10]. In the ITER-FDR, it is considered that the heat load on the first wall due to the TF ripple is not significantly large for a typical operation scenario having a normal shear configuration, but that the heat load is still large for an advanced operation scenario with a reversed shear operation. To avoid the large heat load in the latter case, the installation of ferritic steel has been explored [11].

Though the usefulness of ferromagnetic materials for reducing the loss of energetic ions in a TF ripple was proposed by Turner in 1978 [12], ferromagnetic material was not installed on any tokamak for the purpose of the ripple reduction or for the reduction of energetic ion losses until its installation on the JFT-2M tokamak [13, 14]. (It should be noted that ferritic steel itself was installed on the HT-2 tokamak which was operated in ohmic heating alone [15], not with energetic ions such as neutral beam ions.) In the JFT-2M, two kinds of ripple reductions were carried out. In the first case, ferritic steel was installed between a TF coil and a vacuum vessel outside the vacuum vessel [13]. In the second one, ferritic steel was installed inside the vacuum vessel covering almost the entire inside wall [16]. Low activation ferritic steel is also an attractive material for use as the blanket of a demo-reactor. Thus, another motivation of the second case is to investigate the compatibility of the ferritic steel inside a vacuum vessel and in H-mode plasmas [17]. The ripple was successfully reduced in both cases. As a result of the ripple reduction, a temperature increment on the first wall, which indicates the ripple-induced loss of energetic ions as measured by an infrared TV camera, was also reduced. However, this result was not self-evident because the magnetic structure produced by the ferritic steel was complex due to the limitation of its installation. At that time, the experimental results could not be compared with the simulation, in which the N-folded toroidal symmetry was assumed [18]. Thus, a new version of the OFMC code, the Fully Three-Dimensional magnetic field (F3D) OFMC code, was also developed, in which the three-dimensional complex structure of the toroidal field ripple and the wall shape were included [16].

Through these valuable experiences and results on the JFT-2M, the installation of ferritic steel was proposed on the JT-60U. The main target of this installation on the JT-60U is to utilize large volume plasmas, in which the effect of the TF ripple is large, in order to reach more steady-state, high-beta plasmas, because large volume plasmas benefit from wall-stabilization and from a good coupling with the RF heating/current-drive system. The design work was carried out aiming at an effective, machine-safe, short-

author's e-mail: shinohara.koji@jaea.go.jp

© 2006 The Japan Society of Plasma Science and Nuclear Fusion Research

term installation. In the design work, the enhanced confinement of energetic ions and the absence of unfavorable heat flux on the first wall were assessed by using the F3D OFMC code mentioned above.

Here, we describe how we reached the final design. The procedure of the calculation for positive-ion based neutral beams (PNBs) will be shown in Sec. 2. The calculations were carried out in a large volume configuration because one of the major purposes of ferritic insertion is to operate large volume plasmas with smaller energetic ion loss. The reference case, namely that without ferritic insertion, is shown with the introductive description of the procedure of the calculation in the first subsection in Sec. 2, with three trial cases and a final design also shown in other subsections of Sec. 2. The effectiveness of the final design is also investigated for negative-ion based neutral beams (NNBs) in Sec. 3, and in another plasma configuration with a middle-size volume in Sec. 4. The final section provides a summary.

2. Assessment of Ferritic Inserts in a Large Volume Configuration

2.1 Reference case (TF coils alone)

For the further investigation of the physics in a higher β_N steady-state plasma, we need to utilize the plasma with i) wall stabilization, ii) better RF availability to control a current profile, iii) a source of rotation control to stabilize MHDs such as a resistive wall mode (RWM), and iv) more absorbed heating power. For the first two, we need to use a large volume plasma, which suffers from the large ripple-induced loss in the JT-60U. The ripple-induced loss reduces the confinement of energetic particles, which reduces the heating, current drive, and rotation source. This loss also causes a large heat load on RF antennas. This heat load induces arcing on the antennas and results in the limitation of the pulse length and the coupling between antennas and a plasma. Thus, the available heating or current drive source produced by RF systems is limited. Additionally, due to the ripple-induced loss, a counter rotation is produced even during a perpendicular NBI alone. This counter rotation prevents the peripheral region from the co-rotation, which is expected to be key for obtaining MHD stability and transport in the pedestal region in H-mode plasmas. (It should be noted that in typical plasmas with small ripple loss, perpendicular NBI is utilized for the heating method without inducing rotation.) Thus, it is relatively difficult to control the rotation profile of a plasma with a large ripple-induced loss. Because of these limitations, the usage of large volume plasmas was not a standard operating scenario of the JT-60U.

To overcome these limitations, ferritic insertion for the reduction of the TF ripple was proposed. Through the reduction of the energetic ion loss, the following benefits are expected in the large volume plasma.

1) Improved heating "effective" efficiency. Ripple reduction improves the confinement of NB ions. The ratio of the absorbed power to the deposited power is expected to increase.
2) Extended pulse length and improved efficiency of the RF injection. The large heat load on the RF antennas comes mainly from escaping energetic ions [6, 7]. The reduction of the heat load due to the enhanced confinement of energetic ions will allow improved coupling between antennas and plasma.
3) The availability of the wall stabilization without losing the net heating power due to the enhanced confinement of energetic ions in large volume plasmas.
4) The possibility of enhanced availability of the rotation control to improve MHD stability and transport.

For the above reasons, our basic assessment has been carried out in a large volume plasma configuration, which was that at $t = 3.8$ s of the discharge number E34797 in the JT-60. This plasma configuration is shown in Fig. 1. The strength of the toroidal field was 1.9 T at the machine center of $R = 3.32$ m. Here, the toroidal field was chosen from the following reasons: 1) The thickness of ferritic plates is limited in order to avoid the plasmas coming into direct contact with the ferritic plates. To obtain sufficient ripple reduction from the ferritic plates with a saturation magnetization of about 1.7 T (at 573 K), it is preferable to operate the plasma in a lower toroidal magnetic field. 2) On the other hand, the operation regime of many existing diagnostics and heating systems are optimized in a magnetic field larger than about 2 T. Thus, we decided to assess its installation at 1.9 T, which is one of normal operation points of the toroidal magnetic field in JT-60U.

The calculation was performed by using F3D OFMC

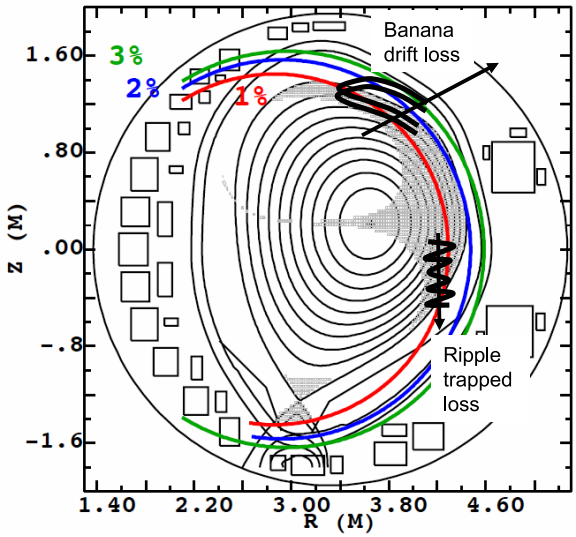

Fig. 1 Plasma configuration with ripple rate contour and ripple well region for TF coils alone, $B_{t_0} = 1.9$ T, $I_p = 1.1$ MA, $q_{95} = 3.4$, plasma volume = 79 m^3, line averaged electron density$\sim 1.5 \times 10^{19}$ m^{-3}, central electron temperature $\sim$ 6 keV, $\beta_N \sim 3$. Schematic view of banana drift loss and ripple-trapped loss is also shown.

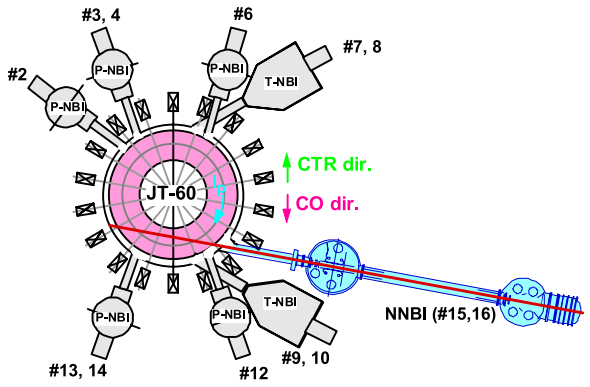

Fig. 2 NB systems on the JT-60U. #2,3,4,6,12,13,14 are perpendicular PNBs. #7,8,9,10 are tangential PNBs. #15,16 are tangential NNBs.

	Absorbed power for full PNBI [%]	Loss power for full PNBI [%]	Absorbed power for perp. PNBI [%]	Loss power for perp.PNBI [%]	Absorbed power for co. PNBI [%]	Absorbed power for ctr. PNBI [%]
w/o FP (subsec 2.1)	50	50	40	60	73	59
"Starting case" (subsec 2.2)	69	31	63	37	87	67
FP on Ceiling (subsec 2.3)	69	31	63	37	87	69
w/o FP on Baffle Board (subsec 2.4)	68	32	61	39	87	68
Final Design (subsec 2.5)	65	35	58	42	84	67

Table 1 Comparison of simulation results for absorbed power and loss power. Power fraction is the ratio to the deposited power in plasma, not to the injection power. (FP: Ferritic Plate)

in order to maintain a consistency in input files for scans, even in the case when the TF pattern maintains an 18-fold toroidal symmetry, such as this reference case. The toroidal-symmetric wall shape is used in the calculation.

The injected neutral beams were 7 perpendicular PNBs, 2 co-tangential PNBs, and 2 counter-tangential PNBs as shown in Fig. 2. The injection energy was 85 keV for this analysis. The total injected power was about 24.75 MW and the deposited power was about 21.5 MW in this case, where the deposited power is the power initially transferred to a plasma by the ionization of neutral beams. The loss power fraction to the deposited power is as shown in Table 1. And the loss power of perpendicularly injected beams is large, i.e., 60% of the deposited power. The distribution of heat flux is presented as an image plot in Fig. 3. The poloidal angle starts from the mid-plane in the low field side. The toroidal angle starts from the "TFC-1" of the JT-60U and increases in the direction of a clockwise direction from the above.

The major loss appears around the mid-plane of the

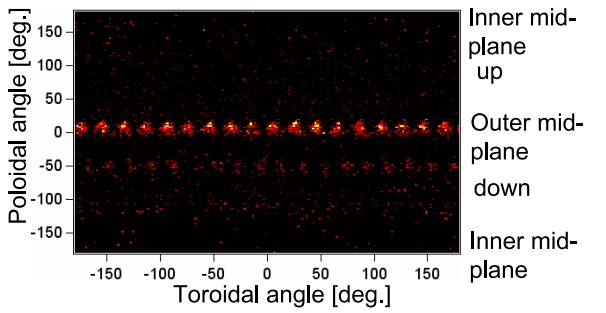

Fig. 3 Distribution of heat flux on the first wall in the reference case. The poloidal angle starts from the mid-plane in the low field side. The toroidal angle starts from the "TFC-1" of the JT-60U and increases in the direction of the clockwise direction from the above.

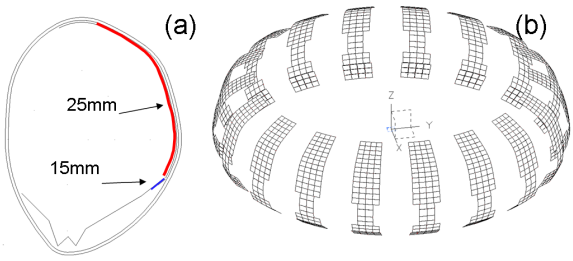

Fig. 4 (a) A poloidal cross section of ferritic inserts under one of TFCs. Note: line thickness is not proportional to the thickness of ferritic steel. The line thickness is exaggerated for illustration. (b) A bird's eye view of the ferritic inserts.

plasma in the lower field side, namely comes from the orbit loss.

In design work, we analyzed several configurations of ferritic insertion. Here, results from three key configurations are described below.

2.2 "Starting case"

In the beginning, we considered only a few important limitations: 1) an installation inside the vacuum vessel because a realistic installation space is not available outside the vacuum vessel. 2) a plate thickness of 25 mm. The thickness should be thinner than carbon tiles of 27 mm in order to avoid the plasma coming into direct contact with the ferritic plates because the ferritic plates partially replace carbon tiles. 3) a typical port shape. The details of the port shape and its interference with diagnostics such as magnetic sensors were not taken into account. These limitations were applied while maintaining the 18-fold toroidal symmetry of the toroidal magnetic field. We then placed ferritic steel as possible on the area where the ripple reduction could effectively be performed based on the map of toroidal field strength.

A poloidal cross section of a ferritic steel installation under one TFC is shown in Fig. 4 (a) and a bird's eye view in Fig. 4 (b). The ferritic material adapted is an 8Cr-2W-

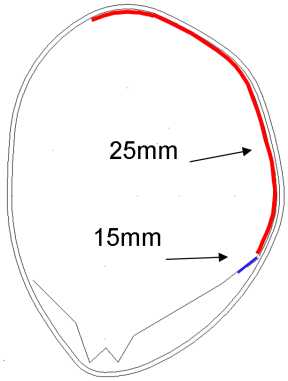

Fig. 5 A poloidal cross section of ferritic inserts under one of TFCs for the case described in Sec. 2.3.

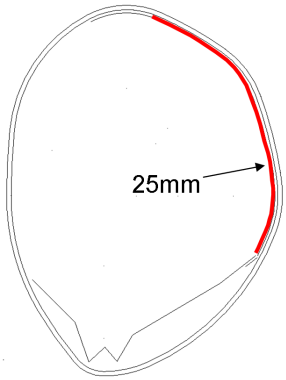

Fig. 6 A poloidal cross section of ferritic inserts under one of TFC for the case described in Sec. 2.4.

0.2V ferritic steel whose saturation magnetization is about 1.7 T at a temperature of 573 K, which is a typical wall temperature in JT-60U operation.

The power loss is reduced from 50% to 31% (Table 1). The reduction of the loss comes mainly from that of the orbit loss.

2.3 Effectiveness of ferritic steel installation on the "ceiling" of the vacuum vessel

A thin region with relatively large ripple amplitude exists on the top of the plasma (Fig. 1), which might induce banana diffusion by enhancing the excursion of the banana tips. In the assessment here, ferritic steel plates were added to the ceiling of the vacuum vessel in order to reduce the ripple in this region, as shown in Fig. 5.

The calculation result is shown in Table 1. Comparing this result with that for the case described in Sec. 2.2, the improvement was small. Additionally, the installation of ferritic plates on the ceiling of the vacuum vessel above plasmas is cost-expensive because the installation could require additional man power and tools such as new cat walks because of the plates heaviness. Thus, we decided not to install ferritic steel on the ceiling.

2.4 Effectiveness of ferritic steel installation on baffle board of divertor

The baffle plate was installed to reduce the backflow of neutral gas in the divertor area [19]. The support structure of the baffle plate has a very small margin of several % to the force on the occurrence of a disruption at B_{t_0}/I_p of 4 T / 3 MA. It is difficult, namely cost-expensive, to place a ferritic plate on the divertor baffle plate because of the additional unfavorable force on a disruption and the heaviness of the ferritic plates. On the other hand, the direction of ion grad B drift is downward when the toroidal magnetic field direction is in the clockwise direction, namely in the case of the normal operation condition of the JT-60U. When the direction of ion grad B drift is downward, the ripple trapped loss is downward. It seems important to reduce ripple amplitude at the downward position in the poloidal cross section. To investigate its effectiveness, we removed the ferritic plates on a part of the divertor baffle, which was installed in the case described in Sec. 2.2. A poloidal cross section for this case is shown in Fig. 6.

The calculation result is shown in Table 1. Comparing this result with that for the case described in Sec. 2.2, the contribution of the ferritic steel on the baffle plate is only 1% for full injection. The reason for this result is considered that in the JT-60U the contribution of the ripple trapped loss is smaller than that of the orbit loss in the large volume plasma because of the positional relation between the plasmas and the first wall.

2.5 Case in consideration of actual technical restrictions with losing 18 fold toroidal symmetry (Final design)

Base on the investigation above, we decided to choose the minimum installation of the case described in Sec. 2.4 as the basis of the final design. In the final design, more realistic technical restrictions were added. These restrictions are: detailed port shapes, e.g., for tangential ports, the interference with diagnostics such as magnetic sensors, and the opposed wall of the NNB injection to avoid accidental heat load. As a result, the 18-fold toroidal symmetry was lost in the magnetic field.

A bird's eye view of the ferritic installation for the final design is shown in Fig. 7 (a). The strength of the toroidal magnetic field at $R = 4.4$ m and $Z = 0.2$ m, where $Z = 0.2$ m is a position of the mid-plane of the typical plasmas in the JT-60U, is also depicted in Fig. 7 (b). The amplitude of the TF ripple is reduced, though the field pattern is complex. For quantitative comparison, the ripple amplitude defined as $(B_{\mathrm{Max}} - B_{\mathrm{min}})/(B_{\mathrm{max}} + B_{\mathrm{min}})$ is not good indicator in this situation. Here, we use the standard deviation normalized by the average, $\delta_{\mathrm{std}} \equiv \sqrt{\langle (B - B_{\mathrm{AVE}})^2 \rangle}/B_{\mathrm{AVE}}$, as an indicator. This value is 0.012 without the ferritic insertion, and 0.006 for the final design case at this position for 1.9 T. The value was reduced by 50% in the final design.

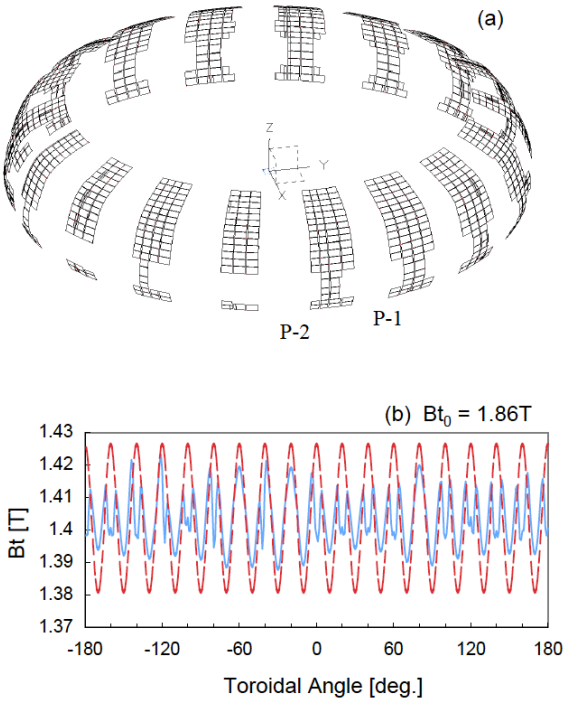

Fig. 7 (a) A bird's eye view of the ferritic inserts in the final design. (b) A toroidal variation of the calculated toroidal magnetic field strength at $R = 4.4$ m and $Z = 0.2$ m. The dotted curve shows the case for TF coils alone, the solid curve shows the case for the final design.

The calculation result is shown in Fig. 8 and Table 1. Compared with the reference case without the ferritic inserts, the absorbed power is increased by about 1.3 times for the full injection of PNB, and the absorbed power of perpendicularly injected beams is increased by about 1.5 times. This result is strongly encouraging for the possibility of increasing the availability of the rotation control by using tangential NBs, keeping the absorbed heating power similar to the previous high performance discharges by using perpendicular NBs alone.

As is written above, one of the important objectives of this installation is the reduction of the heat load onto the LH antennas. We also estimated the heat load on the LH antenna region. The heat load onto the antennas was reduced from 0.55 MW/m^2 to 0.2 MW/m^2 in this calculation of full PNB injection. It is expected that the duration of an LH injection can be expanded more than twice. Additionally, we have confirmed the absence of the unfavorable heat flux on the first wall. Namely, the observed heat load was less than the acceptable level of about 2 MW/m^2.

The magnetic field produced by ferritic plates is saturated above the external vacuum magnetic field of about 0.6 T. The magnetic field produced by ferritic plates is almost constant in the typical operational toroidal magnetic field, namely > 1 T, on the JT-60U. This means that the ferritic plates might "over-cancel" the TF ripple in the lower magnetic field and work less effectively in the higher mag-

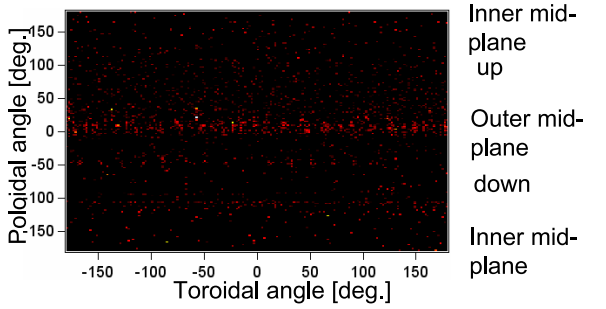

Fig. 8 Distribution of heat flux on the first wall in the final design. The range of index color mapping is same with Fig. 3.

netic field. It is interesting to check the effectiveness of the ferritic insert in the different strengths of the magnetic field produced by TFCs. We have assessed the effectiveness in the different strengths of the magnetic field of 1.2 T, 1.6 T, 2.6 T and 3.3 T. Most of the plasma parameters are the same as those indicated in Fig. 1. The plasma current and poloidal coil current varied depending on the value of the toroidal field. Namely, the profile of the safety factor, q, is identical to the case shown in Fig. 1. The strengths of the toroidal magnetic field at $R = 4.4$ m and $Z = 0.2$ m are depicted for these 4 cases in Fig. 9. The ripple amplitude for 2.6 T and 3.3 T is reduced less compared with the case of 1.9 T; however, we can see the reduction of the ripple amplitude. Figure 10 shows the variation of the absorbed power fraction for cases with and without the ferritic insertion and the ratio of the absorbed power with the ferritic insertion to that without the ferritic insertion. The ferritic insertion is less effective for the cases of 2.6 T and 3.3 T, compared with 1.2, 1.6, and 1.9 T. Even so, the absorbed power was enhanced by about 1.2 for both the cases of 2.6 T and 3.3 T. Interestingly, the enhancement of the absorbed power was still observed for 1.2 T in this configuration, though the over-cancel can be observed at the position of the TF coils, as seen in the peaks of the dotted curve in Fig. 9.

3. Effectiveness of Ferritic Inserts on Negative-Ion Based Neutral Beams

In the JT-60U, the NNB system (Fig. 2) is operated as a high energy beam source of 300 – 420 keV. Because of its high energy, some aspects are utilized to simulate alpha particles. One example is experiments regarding Alfven eigenmodes [20, 21]. The tangency radius, R_{tan}, of the NNB beam line is 2.6 m, while the major radius of the vacuum vessel is 3.32 m. The direction of the injection is in the same direction as the plasma current and toroidal field. Therefore, most of the beam ions are co-passing ions. Thus, though it was expected that the effect of the rippled toroidal field was small, the effectiveness of the ferritic insert was investigated for the final design case because the beam energy was large. The results of the comparison at

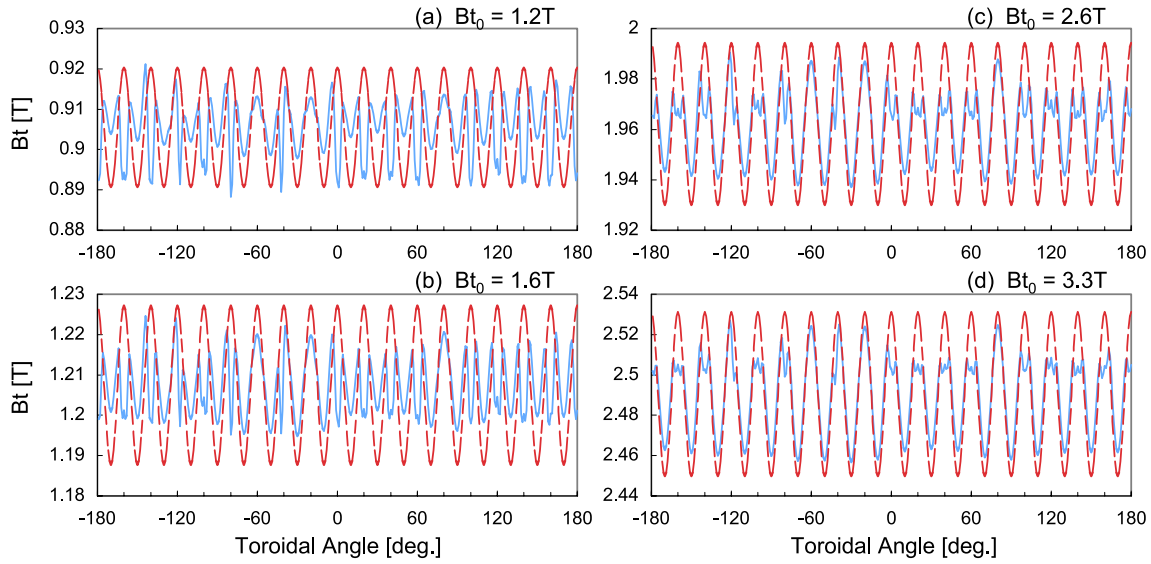

Fig. 9 Toroidal variation of the calculated toroidal magnetic field strength at $R = 4.4$ m and $Z = 0.2$ m. The dotted curve shows the case for TF coils alone, the solid curve shows the case for the final design. (a) for $B_{t_0} = 1.2$ T, (b) for $B_{t_0} = 1.6$ T, (c) for $B_{t_0} = 2.6$ T, (d) for $B_{t_0} = 3.3$ T.

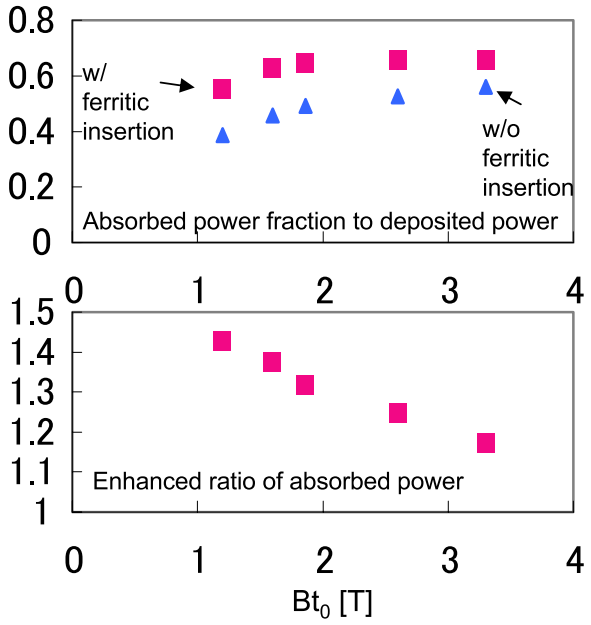

Fig. 10 Variation of the absorbed power fraction for cases with and without ferritic inserts, and the ratio of the absorbed power with ferritic inserts to that without ferritic inserts.

1.9 T are shown in Table 2. The ferritic insert is still effective for this high energy beam source, the NNB.

In this co-tangeintial NNB injection, most birth ions, > 99%, are transit ions. It is expected that this improvement comes mainly from the banana ions produced by pitch angle scatterings in the slowing down process. Thus, the contribution of the ion heating might be increased in the absorbed power. It is interesting to evaluate the enhanced contribution of ion heating in the NNB injection, which heats mainly electrons. We have evaluated these contributions. The contribution of ion heating power to

	Absorbed power for co NNB [%]	Loss power for co NNB [%]
w/o FP (subsec 2.1)	75	25
Final Design (subsec 2.5)	84	16

Table 2 Comparison of simulation results for NNB.

the absorbed power has changed from 23% to 25%. This increase is small, which means banana ions still have high energy and can collide mainly with electrons rather than with ions.

4. Effectiveness of Ferritic Inserts in a Middle-size Volume Configuration

In the large volume plasmas analyzed above, the major loss is the orbit loss around the mid-plane of the plasmas. Thus, it is considered that the final design, in which most of the ferritic plates are installed above the mid-plane, is effective in the large volume plasma. However, it was not obvious whether such an installation was effective in a middle-size volume plasma, in which the ripple-trapped loss appears clearly.

We have investigated the effectiveness of ferritic insertion of the final design in a middle-size volume configuration of $B_{t_0}/I_p = 1.9\,\mathrm{T}/1.1\,\mathrm{MA}$. The plasma configuration is shown in Fig. 11. All of the injected beams are PNBs. The results of the comparison are shown in Table 3. The ferritic inserts of the final design work even in the case of the middle-size configuration. Without the ferritic inserts,

heat loads exist on the first wall of the downward position of the plasma. These heat loads come from the ripple-trapped loss. The ferritic inserts greately reduced these heat loads. It is considered that the ferritic plate around the mid-plane of the vacuum vessel can effectively reduce the TF ripple on some low-field-side position of the plasma, distant from the ferritic plates. Figure 12 shows a "quasi" ripple well map. Because of the complex ripple structure, we cannot use the α-parameter, $\alpha \equiv r/NRq\delta$, to determine the ripple well structure. Here, we define a "quasi" ripple well at a toroidal angle (φ_s) if there is a local minimum of the magnetic field within $\varphi_s - \Delta\varphi < \varphi < \varphi_s + \Delta\varphi$, where $\Delta\varphi$ is half of the period of the TF coil installation. It is confirmed that the ripple well region, which plays an important role on the ripple-trapped loss mechanism, is reduced after the ferritic insertion. This result is similar to the experimental results of the external ferritic plate installation on the JFT-2M [16].

5. Summary

In further pursuit of the steady-state advanced tokamak research, a ferritic insertion was proposed to reduce the TF ripple. The ripple reduction in large volume plasmas is expected to bring 1) improved heating "effective" efficiency, 2) extended pulse length and improved efficiency of the RF injection, 3) the availability of wall stabilization without losing heating power, and 4) the possibility of enhanced availability of rotation control to improve MHD stability and transport. This proposal regarding ferritic insertion is based on its success in the ferritic insert program of the JFT-2M. In the design process concerning ferritic insertion, the confinement of energetic ions and the absence of the unfavorable heat flux on the first wall was assessed by using the F3D OFMC code, which was developed for the ferrite insert project in the JFT-2M.

A large volume plasma of $B_{t_0}/I_p = 1.9\,\mathrm{T}/1.1\,\mathrm{MA}$ was investigated in order to determine the final configuration of the installation. In the final design, the absorbed power in the neutral beam injection is improved by a factor of about 1.3 for PNBI and about 1.1 for NNBI. We also assessed the effectiveness of the ferritic insertion on toroidal fields of the several different strengths. Some benefits of ferritic insertion can be available at higher values of the toroidal magnetic field. A medium-sized plasma was also analyzed. The ripple-trapped loss was reduced and the confinement of energetic ions was improved by about 1.1 for PNBI. These results are encouraging for our coming experiments.

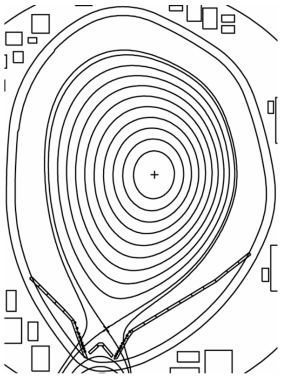

Fig. 11 Plasma configuration assessed for a middle-size volume. $B_{t_0} = 1.9\,\mathrm{T}$, $I_p = 1.1\,\mathrm{MA}$, $q_{95} = 2.93$, plasma volume = $67.5\,\mathrm{m}^3$, line averaged electron density $\sim 2.2 \times 10^{19}\,\mathrm{m}^{-3}$, central electron temperature $\sim 4\,\mathrm{keV}$, $\beta_N \sim 1.9$.

	Absorbed power for full PNBI [%]	Loss power for full PNBI [%]	Absorbed power for perp. PNBI [%]	Loss power for perp. PNBI [%]	Absorbed power for co. PNBI [%]	Absorbed power for ctr. PNBI [%]
w/o FP	69	31	60	40	92	76
Final Design	79	21	73	27	95	78

Table 3 Comparison of simulation results for a middle-size volume configuration.

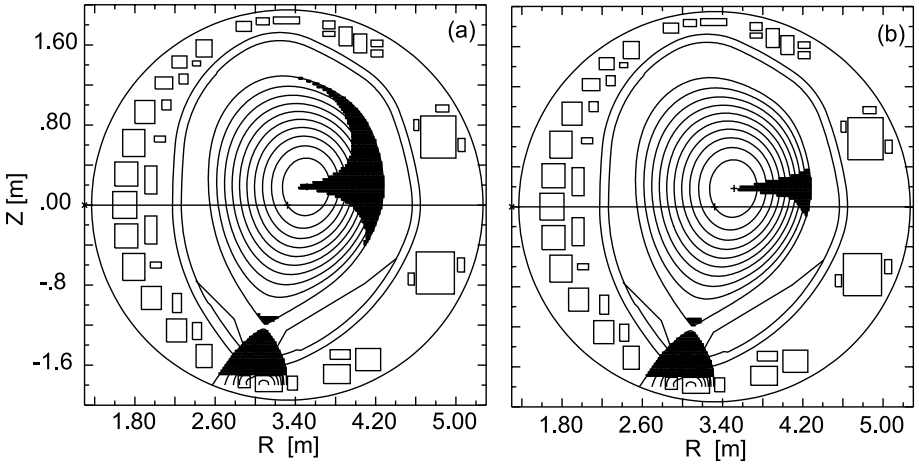

Fig. 12 "Quasi" ripple well map around Port No. 1 (P-1) section before the ferritic insertion (a) and after the insertion (b).

Acknowledgment

We would like to acknowledge the support and useful comments of Dr. K. Tani, Dr. K. Tobita, and Dr. Y. Kamada of the JAEA. We also would like to thank Mr. M. Suzuki of the CSK Corporation for his support in the development of the F3D OFMC code.

[1] JET TEAM (presented by B.J.D. Tubbing), "*The impact of increased toroidal field ripple in JET", Plasma Physics and Controlled Nuclear Fusion Research 1992 (Proc. 14th Int. Conf. Würzburg)*, IAEA-CN-56/A-7-5.
[2] ITER Physics Expert Group on Energetic Particles, Nucl. Fusion **39**, 2471 (1999).
[3] V. Basiuk *et al.*, Nucl. Fusion **44**, 181 (2004).
[4] K. Tobita *et al.*, Nucl. Fusion **35**, 1585 (1995).
[5] R.B. White *et al.*, *Plasma Phys. and Controll. Nucl. Fusion Research 1988 (Proc. 12th Int. Conf. Nice)* IAEA, Vienna (1989) Vol. 2. 111.
[6] V. Ya. Goloborod'ko *et al.* Physica Scripta T**16**, 46 (1987).
[7] K. Tani *et al.*, *Plasma Phys. and Controll. Nucl. Fusion Research 1988 (Proc. 12th Int. Conf. Nice)* IAEA, Vienna (1989) Vol. 2. 121.
[8] E. Bittoni and M. Haegi, Fusion Technol. **18**, 373 (1990).
[9] S.V. Putvinskij *et al.*, Nucl. Fusion **34**, 495 (1994).
[10] S.V. Konovalov. *et al.*, '*Energetic particle ripple loss in ITER*', *in Proc. 28th EPS Conf. on Controlled Fusion and Plasma Physics*, Funchal-Madeira, Portugal (2001).
[11] K. Tobita, T. Nakayama, S.V. Konovalov and M. Sato, Plasma Phys. Control. Fusion **45**, 133 (2003).
[12] L.R. Turner, S-T. Wang and H.C. Stevens, *Iron shielding to decrease toroidal field ripple in a tokamak reactor, Proc. 3rd Topical Meeting on Technology of Controlled Nuclear Fusion* (Santa Fe, 1978) p.883.
[13] H. Kawashima, M. Sato, K. Tsuzuki, Y. Miura, N. Isei, H. Kimura, T. Nakayama, M. Abe, D.S. Darrow and JFT-2M Group, Nucl. Fusion **41**, 257 (2001).
[14] K. Shinohara *et al.* Fusion Technol. (*accepted*)
[15] T. Nakayama, M. Abe, T. Tadokoro and M. Otsuka, J. Nucl. Mater. **271&272**, 491 (1999).
[16] K. Shinohara, H. Kawashima, K. Tsuzuki, K. Urata, M. Sato, H. Ogawa, K. Kamiya, H. Sasao, H. Kimura, S. Kasai, Y. Kusama, Y. Miura, K. Tobita, O. Naito, the JFT-2M Group and D.S. Darrow, Nucl. Fusion **43**, 586 (2003).
[17] K. Tsuzuki, H. Kimura, H. Kawashima *et al.*, Nucl. Fusion **43**, 1288 (2003).
[18] K. Tani, T. Takizuka and M. Azumi, J. Plasma Fusion Res. **66**, 35 (1991).
[19] N. Hosogane, H. Tamai, S. Higashijima *et al.*, J. Nucl. Mater. **266-269**, 296 (1999).
[20] K. Shinohara *et al.*, Nucl. Fusion **42**, 942 (2002).
[21] K. Shinohara *et al.*, J. Plasma Fusion Res. **81**, 547 (2005).